Characterizing acoustic shocks in high-performance jet aircraft flyover noise

Brent O. Reichman, Kent L. Gee, Tracianne B. Neilsen, J. Micah Downing, Michael M. James, Alan T. Wall, and Sally Anne McInerny

Citation: The Journal of the Acoustical Society of America **143**, 1355 (2018); doi: 10.1121/1.5026026

View online: https://doi.org/10.1121/1.5026026

View Table of Contents: http://asa.scitation.org/toc/jas/143/3

Published by the Acoustical Society of America

Characterizing acoustic shocks in high-performance jet aircraft flyover noise

Brent O. Reichman,[a] Kent L. Gee, and Tracianne B. Neilsen
Department of Physics and Astronomy, Brigham Young University, N283 ESC, Provo, Utah 84602, USA

J. Micah Downing and Michael M. James
Blue Ridge Research and Consulting, LLC, Asheville, North Carolina 28801, USA

Alan T. Wall
Air Force Research Laboratories, Battlespace Acoustics Branch, 2610 Seventh Street, Building 441, Wright-Patterson Air Force Base, Ohio 45433, USA

Sally Anne McInerny
Department of Mechanical Engineering, University of Louisiana at Lafayette, Rougeou Hall, Room 320, Lafayette, Louisiana 70504, USA

(Received 4 October 2017; revised 9 February 2018; accepted 14 February 2018; published online 6 March 2018)

Acoustic shocks have been previously documented in high-amplitude jet noise, including both the near and far fields of military jet aircraft. However, previous investigations into the nature and formation of shocks have historically concentrated on stationary, ground run-up measurements, and previous attempts to connect full-scale ground run-up and flyover measurements have omitted the effect of nonlinear propagation. This paper shows evidence for nonlinear propagation and the presence of acoustic shocks in acoustical measurements of F-35 flyover operations. Pressure waveforms, derivatives, and statistics indicate nonlinear propagation, and the resulting shock formation is significant at high engine powers. Variations due to microphone size, microphone height, and sampling rate are considered, and recommendations for future measurements are made. Metrics indicating nonlinear propagation are shown to be influenced by changes in sampling rate and microphone size, and exhibit less variation due to microphone height.
https://doi.org/10.1121/1.5026026

[DKW] Pages: 1355–1365

I. INTRODUCTION

Community annoyance of military aircraft noise is due not only to the high sound levels associated with high-performance jet noise, but may also be influenced by its sound quality. One component of the noise, crackle,[1] is the perception of acoustic shocks within the waveform.[2] Due to nonlinear propagation, these shocks and the high-frequency energy associated with them persist to distances greater than expected under linear assumptions.[3,4] The nonlinear propagation of jet noise serves to steepen the waveform and form shocks, even well away from the source. Nonlinear propagation was originally identified as an explanation for the lack of atmospheric absorption in far-field full-scale jet data[5,6] and has since been confirmed through numerical modeling.[7] Modeling efforts have shown the effects of nonlinear propagation in both the temporal[8–10] and frequency[11,12] domains.

Many of the attempts to quantify the effects of nonlinear propagation in jet noise waveforms have revolved around statistical quantities. When the phenomenon of crackle was first discussed by Ffowcs-Williams *et al.*,[1] the skewness of the pressure waveform was proposed as a metric indicating the presence of crackle, a measure that is still in use today.[13,14] However, since crackle is associated with the presence of shock waves, which have large positive derivative values, more recent work has shown that the skewness of the first time derivative of the pressure waveform, or derivative skewness, is more connected to the presence of shock waves and crackle.[15,16] The derivative skewness has since been used to show the steepened nature of nonlinearly propagated jet noise.[17,18] Other quantities, such as the average steepening factor (ASF)[19,20] or frequency-based metrics have also been used to quantify nonlinear effects.[5,8] Most of these studies utilize data collected in static jets or ground run-ups with a tethered aircraft.[21,22]

Forward flight can significantly change the noise source, but the impact of flight effects is not completely understood, in particular with regards to nonlinear propagation. Several significant studies have compared jet noise measured during flyover operations with ground run-ups or lab-scale tests. As early as the 1970s, spectra were measured during flyover events,[23] and later noise predictions were made based on static measurements.[24] Krothapalli *et al.*[25] subsequently performed model-scale tests in a wind tunnel to simulate forward flight of a heated supersonic jet and found the wind caused changes in far-field noise. Schlinker *et al.*[26] performed similar tests with installed chevrons to observe noise reduction. In recent full-scale work regarding flyover measurements, Seiner *et al.*[27] used a linear array of microphones to obtain narrowband spectra and validate noise predictions

[a]Electronic mail: brent.reichman@gmail.com

for F-18 flyover operations. In more recent work, Michel[28] analytically predicted the effects of forward flight on mixing noise, resulting in an increase in level due to "stretching of the flow field of the jet."

Fewer analyses exist examining the nonlinear characteristics of jet noise while in flight.[5,29] McInerny *et al.*[30] used a combination of time-domain and spectral methods to inspect flyover data for evidence of nonlinear propagation and to investigate effects of microphone height from ground level up to 11.9 m (39 ft) above ground level. They concluded that characteristics indicative of nonlinear propagation are seen in flyover data, and that microphones should be placed off the ground to ensure cleaner measurements.

This paper considers the nonlinear propagation of jet noise produced by an F-35 aircraft during flyover operations. The analyses begin by considering spectra, waveforms, derivatives, and their probability density functions (PDFs) at low and high-power engine conditions. Various time-domain nonlinearity metrics are calculated for individual waveforms over multiple measurement conditions, showing time-domain evidence of nonlinear propagation at high-power conditions. Behavior of these metrics as a function of microphone size and height and sampling rate show that these measurement parameters impact the various metrics differently. Recommendations are given for future measurements and recommendations are made for standard practices[31] for high-performance military jet noise measurements.

II. NONLINEARITY METRICS

To discuss nonlinearity and shock formation for noise waveforms, the behavior of the entire waveform must be taken into account. To gauge overall waveform behavior, metrics are often based on the probability distribution function (PDF) of the waveform or its derivative.[8,15,32] Two such metrics are used in this analysis: the skewness of the first time derivative of the pressure waveform, also known as the derivative skewness, and the ASF.

The skewness of a distribution expresses asymmetry of the PDF and accentuates outliers due to the cubed nature of the numerator. The skewness of a zero-mean variable x is defined as

$$\mathrm{Sk}\{x\} = \frac{E[x^3]}{E[x^2]^{3/2}}, \tag{1}$$

where $E[x]$ represents the expectation value of x. A skewness value of zero represents a symmetric distribution, while a positive number indicates the presence of a higher number of large positive values than negative. The skewness of the pressure waveform was initially used to quantify crackle, an auditory phenomenon associated with shock waves within jet noise.[1] However, to quantify shocks themselves it is more useful to use the derivative skewness, which refers to the skewness of the PDF of the first time derivative of the waveform and expresses an asymmetry in derivative values. The derivative skewness accentuates the large derivatives (rapid pressure increases) associated with shock waves and is indicative of shocks forming due to nonlinear propagation.[16] It has been shown that a derivative skewness value greater than five is indicative of significant shocks within a waveform.[33]

The ASF[19] is also based on derivative values and defined as the average value of the positive derivatives over the average value of the negative derivatives:

$$\mathrm{ASF}\{p\} = \frac{E[\dot{p}^+]}{E[\dot{p}^-]}. \tag{2}$$

The ASF, which is an inverse of the previously used Wave Steepening Factor,[34] is a linear average of derivative values, which makes it less sensitive to outliers than the derivative skewness, and thus better represents average behavior. An ASF value of one represents a waveform with no significant steepening, while a value above one represents some nonlinear steepening.[19] It has been shown that for jet noise, both full-scale[35] and model-scale,[18] that an ASF value between 1.5 and 2 is indicative of the presence of shocks, with a value approaching two suggesting significant shock content.

III. FLYOVER MEASUREMENT SETUP

The dataset considered was part of a larger measurement of F-35 flyover events at Edwards Air Force Base in 2013. The data shown are from the F-35A but are representative of the F-35B as well.[36] The F-35A flew between two cranes, one located 305 m (1000 ft) north of the flight path, and one located 305 m (1000 ft) to the south. Flights were performed at several engine conditions, ranging from 15% engine thrust request (ETR) to 150% ETR. The height of the aircraft varied during each measurement, with some constant altitude flights at 76, 152, and 305 m (250, 500, and 1000 ft) and other flights with the aircraft climbing to maintain constant velocity at high engine power conditions.

Measurements were performed according to ANSI S12.75,[31] which outlines procedures for full-scale military aircraft noise measurements in both static and flyover cases. While this standard involves calculating directivity of the noise and requires microphones at various locations, one of the purposes of this paper is to highlight differences due to measurement considerations. The measurement involved microphones of different sizes, heights and locations around the aircraft. However, at the north tower redundant 1/2 and 1/4 in. microphones were placed at several heights between 0 and 91 m, giving an ideal comparison. Thus, to reduce other variations and highlight the differences in question, this paper concentrates on microphones from the north crane, located 305 m (1000 ft) from the flight path of the aircraft. Prepolarized pressure microphones from G.R.A.S. Sound and Vibration were suspended at various heights from a caving ladder hanging off of the crane, as shown in Fig. 1. All microphones were pointed directly up, giving a nearly perpendicular angle of incidence ($\pm 15^\circ$) as the aircraft flew by at a height of 76 m (250 ft), ideal for measurements with pressure microphones to ensure accurate estimation of shock amplitude.[37] At several heights, specifically 0, 9.1, 30.5, 61.0, and 91.4 m (0, 30, 100, 200, and 300 ft), two microphones were placed side by side, roughly 0.13 m (6 in.) apart. The two microphones consisted of one 40BD 6.35 mm (1/4 in.) microphone[38] with a 26CB preamplifier and

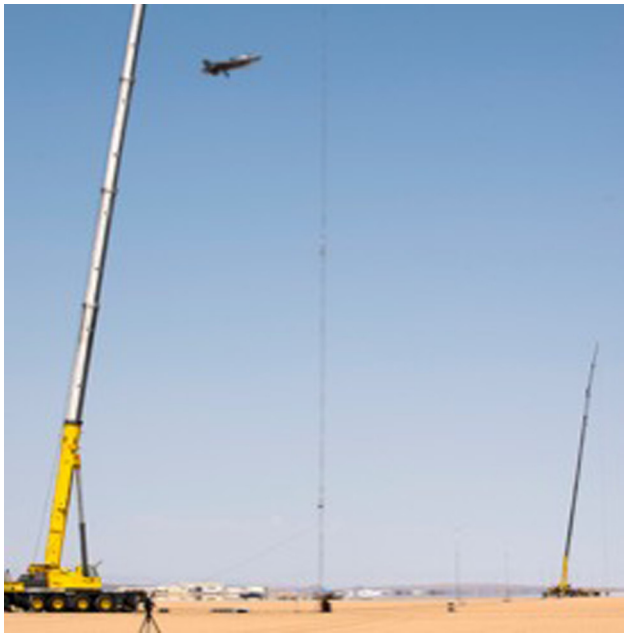

FIG. 1. (Color online) An F-35 flying between two cranes, each located 305 m (1000 ft) from the flight path of the aircraft. Microphones were hung from the 91.4 m cranes at multiple heights, with five heights having redundant 1/2 and 1/4 in. microphones.

one 46AO 12.7 mm (1/2 in.) microphone.[39] The 40BD microphones have a flat frequency response within 2 dB up to 70 kHz and the 46AO microphones up to 20 kHz. Though wind speeds were low (4 knots or less) during flyover events the 1/2 in. microphones had wind screens placed on them. Temperatures during the measurement ranged from 16.3 °C to 34.6 °C. Relative humidity ranged from 17.3% to 37.7%, while atmospheric pressure remained nearly constant at 0.92 atm.

IV. CHARACTERIZING NONLINEARITY IN FLYOVER WAVEFORMS

Evidence of nonlinear propagation can be found in individual waveform segments as well as statistical measures that represent the entire event. In the remainder of this paper, evidence for nonlinear propagation is found by comparing waveforms and their derivatives between engine conditions. The presence of shock waves in the waveforms themselves is shown, as well as statistical measures indicating the overall steepness of the waveforms. Waveforms and statistics are compared for both low and high-power operating conditions. The comparison is presented for a 1/4 in. microphone located 91 m (300 ft) above the ground. The distance from this microphone to the aircraft, $r(t)$, and the angle of the microphone relative to the nose of the aircraft, θ, are shown for example flyover events in Fig. 2. The aircraft position is plotted relative to the time t, with $t = 0$ representing the point of closest approach between the aircraft and microphone. For both the low and high-power cases the aircraft was flying 76 m (250 ft) above ground level, giving a point of closest approach of roughly 305 m.

A. Waveforms and derivatives

A comparison of characteristics of waveforms measured at various ETR settings allows for a clear indication of

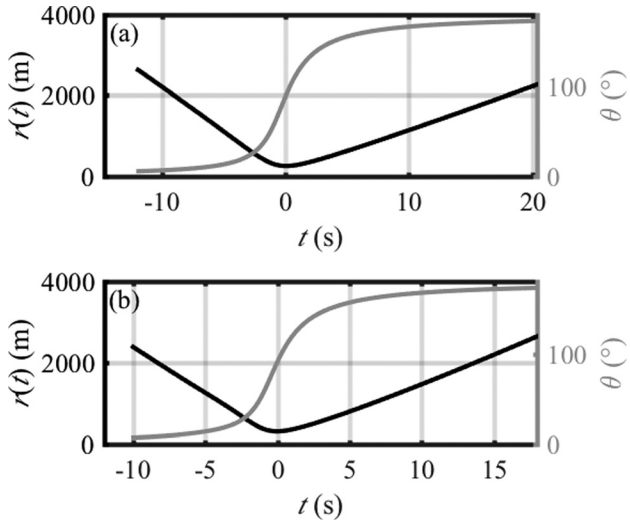

FIG. 2. The distance from the microphone to the aircraft $r(t)$ and angle of the microphone relative to the nose of the aircraft $\theta(t)$ for example flyover events at (a) 55% ETR and (b) 150% ETR. This microphone was located 91.4 m above ground level, hung from a crane located 305 m north of the flight path of the aircraft.

nonlinear behavior. A sample of each waveform at the time of maximum overall sound pressure level (OASPL) is shown in Fig. 3(a) for 55% ETR and in Fig. 3(b) for 150% ETR. The peak pressures increase by nearly a factor of 10 from the 55% ETR case to 150% ETR case. In addition to the increase in pressure, sharp compressive pulses are seen for

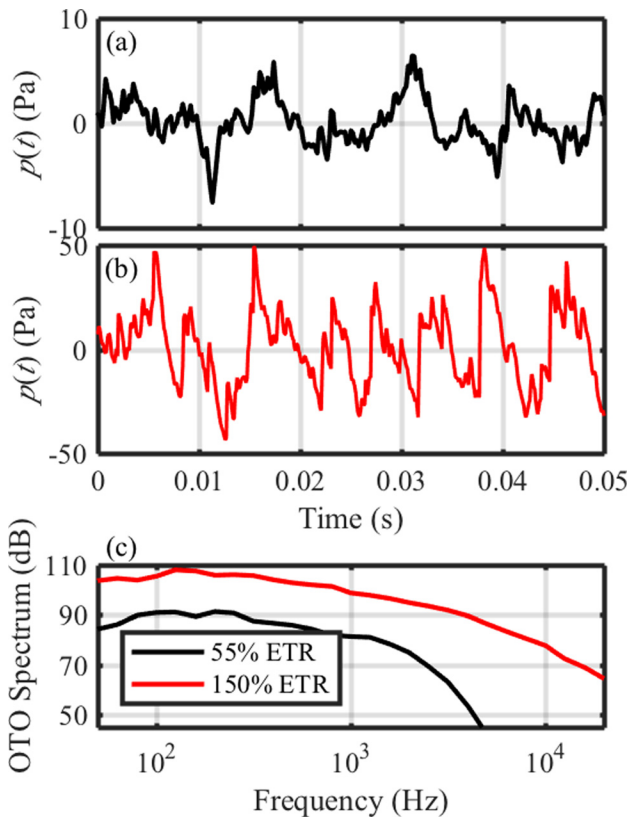

FIG. 3. (Color online) Waveforms from (a) 55% ETR, (b) 150% ETR, and (c) the spectra from each. Sharp compressions, or shock waves, are seen in the high-power waveform and produce the relative increase in high-frequency content.

150% ETR: The pressure increases dramatically over a short period of time. These steepened sections of the waveform are shocks, sharp increases in pressure occurring over a period on the order of tens of microseconds. Shocks have a significant impact on the spectrum, shown in Fig. 3(c), calculated over the 0.5-s block containing the maximum OASPL. At this distance, over 300 m from the aircraft, atmospheric absorption at high frequencies has a large effect. This is evident at 55% ETR, as the high-frequency levels decrease exponentially above 1 kHz. However, at 150% ETR, the spectral shape has changed dramatically. Although the spectrum peaks at roughly the same frequency as at 55% ETR, the same high-frequency roll-off is not observed. This apparent lack of atmospheric absorption is what initially led Pernet and Payne,[4] and later Morfey and Howell,[5] to suspect that nonlinear propagation had a significant spectral effect on jet noise.

B. Flyover waveforms

Although individual shocks at over 300 m from the aircraft show the steepened nature of flyover waveforms, characteristics of the entire waveform are needed to gauge overall trends. The waveform from the entire 55% ETR flyover event, its time derivative, and their respective probability density functions are shown in Fig. 4, for the same microphone used in Fig. 3. The pressure waveform is shown in Fig. 4(a), with the 6-dB down region highlighted in black. [The 6-dB down region contains the times when the root mean square (rms) level is within 6 dB of the peak rms level.] At this distance and low engine power, the pressure peaks near 10 Pa, with a symmetric distribution centered around 0 Pa. The time derivative of the waveform, shown in Fig. 4(c), appears skewed, with negative values reaching −20 kPa/s and positive values reaching approximately 35 kPa/s. The difference between these two distributions is more obviously seen in the plots of the PDF (Ref. 40) of the 6-dB down portion of the waveform and its derivative, shown in Figs. 4(b) and 4(d), respectively. These plots are shown with respect to σ_p and $\sigma_{\partial p/\partial t}$, the standard deviation of the pressure waveform and its derivative, respectively. While the PDF of

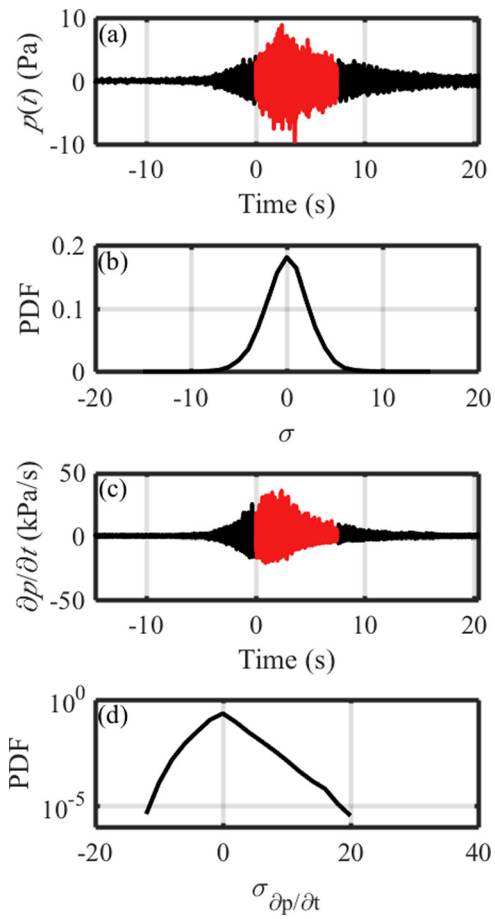

FIG. 4. (Color online) (a) The waveform measured at a location 305 m away from an F-35A flying at 55% ETR at 76.2 above the ground. (b) The PDF of the 6-dB down portion of the waveform, shown as a function of the pressure standard deviation σ. (c) The time derivative of the waveform. (d) The PDF of the derivatives from the 6-dB down portion of the waveform as a function of the derivative standard deviation $\sigma_{\partial p/\partial t}$.

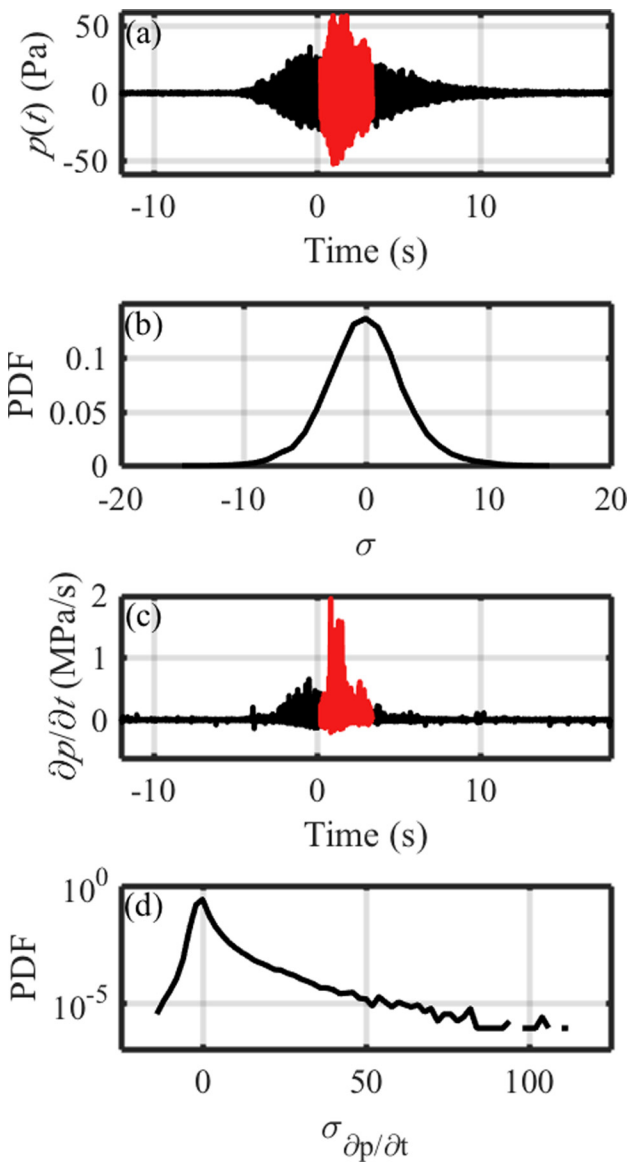

FIG. 5. (Color online) (a) The waveform measured at a location 305 m away from an F-35A flying at 150% ETR at 76.2 m above the ground. (b) The PDF of the 6-dB down portion of the waveform. (c) The time derivative of the waveform. (d) The PDF of the derivatives from the 6-dB down portion of the waveform.

the pressure waveform is roughly symmetric about 0, the PDF of the derivative shows larger positive derivatives than negative. Though the slightly skewed PDF of the derivative suggests that waveforms are steepened, the difference between positive and negative derivative values is not large enough to suggest the presence of acoustic shocks.[33]

Contrasting waveforms between different engine conditions confirms the presence of nonlinear propagation at high-power engine settings. Figure 5 shows a waveform from the same microphone as Fig. 4, but with the aircraft operating at 150% ETR instead of 55%. At 150% ETR, the pressure waveform amplitude reaches values more than five times that of the lower power setting, over 50 Pa, but the starkest difference is in the derivative values. The greatest positive derivative values peak at 2 MPa/s, and although the pressure waveform PDF shown in Fig. 5(b) is still nearly symmetric about 0 Pa as in far-field ground run-up measurements,[41] the PDF of the waveform derivative shows a much higher positive asymmetry, with some positive derivative values reaching over 100 standard deviations.

C. Metrics characterizing nonlinear propagation

The quantities discussed in Sec. II—the derivative skewness and ASF—are calculated along with OASPL from the 0.5 s blocks of the waveforms shown in Figs. 4 and 5. These statistics are investigated as a function of time, with 80% overlap between blocks, and are shown in Fig. 6 for 55% ETR. Figure 6(a) shows the OASPL as a function of time, with the OASPL peaking shortly after the aircraft passes over. The derivative skewness and ASF of Fig. 6(b) and 6(c), respectively, both peak within this 6-dB down region, indicating steepened waveforms. The low value of the peak of the derivative skewness at $\mathrm{Sk}\{\partial p/\partial t\} = 0.8$ indicates that the waveform is steepened but does not contain significant shocks.[33] The peak ASF value of 1.22 confirms this assessment, suggesting steepened waveforms but not the presence of shocks throughout the 6-dB down region of the waveform. Thus, for this low-power case at 55% ETR, most of the statistics confirm conclusions drawn from the waveform and its PDF. Figure 6(d) shows the position of the aircraft as a function of time, including both the distance $r(t)$ and the angle of the microphone with respect to the aircraft nose, $\theta(t)$. The OASPL, derivative skewness, and ASF all peak shortly after the point of closest approach, at an angle of approximately 140° due to the directivity of the jet noise source.

In contrast with the lower-power case, high-power flight results in the presence of acoustic shocks. Figure 7 shows statistics of the waveform from Fig. 5, when the aircraft is

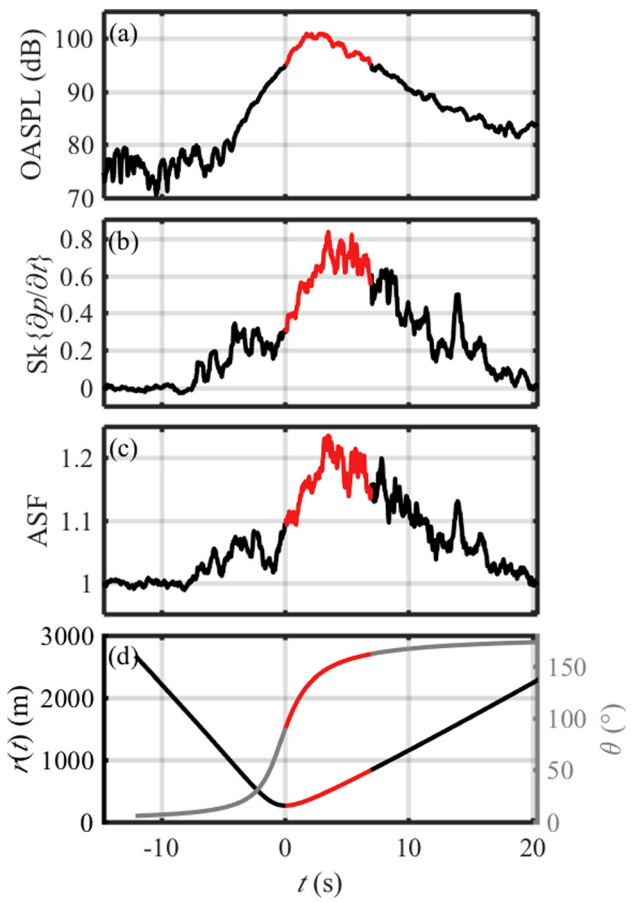

FIG. 6. (Color online) Statistics of the 55% ETR flyover waveform shown in Fig. 4(a), specifically the (a) OASPL, (b) derivative skewness, (c) ASF, and (d) the distance from the aircraft to the microphone, $r(t)$ and the angle of the microphone relative to the aircraft nose, $\theta(t)$. The 6-dB down region is highlighted in parts (a)–(c).

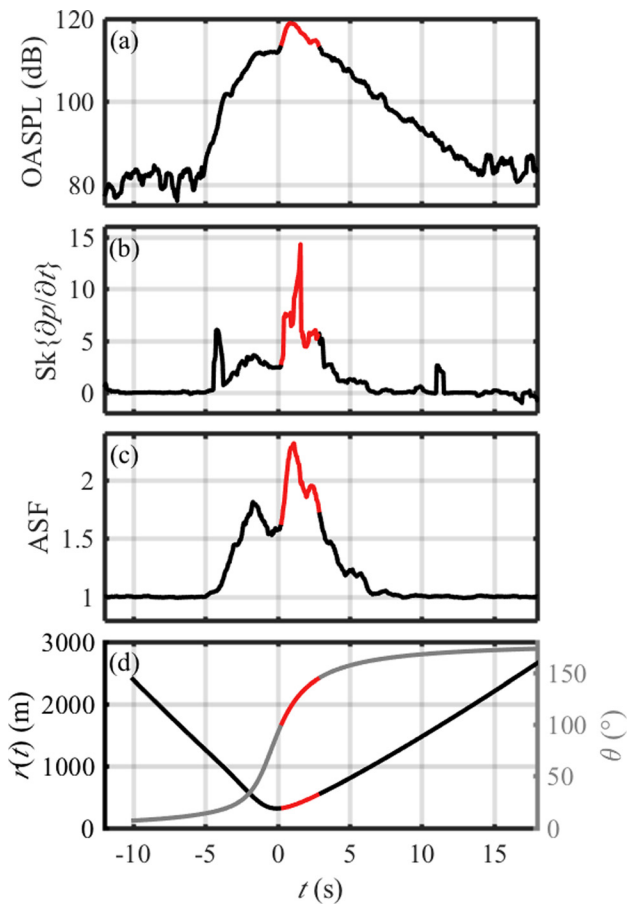

FIG. 7. (Color online) Statistics of the 150% ETR flyover waveform in Fig. 5(a), specifically the (a) OASPL, (b) derivative skewness, (c) ASF, and (d) the distance from the aircraft to the microphone, $r(t)$ and the angle of the microphone relative to the aircraft nose, $\theta(t)$. The 6-dB down region is highlighted in parts (a)–(c).

operating at 150% ETR. The derivative skewness in Fig. 7(b) reaches much higher values during this event, up to $Sk\{\partial p/\partial t\} = 14.3$, indicating the presence of significant shocks, even at 305 m from the aircraft flight path. The ASF also shows a higher peak in Fig. 7(c), with a value of 2.4 for the high-power case, indicative of significant shock content, versus 1.22 for the low-power case. Since the ASF is a ratio of positive derivatives to negative, a Gaussian waveform has an ASF of 1, meaning an ASF of 2.4 is much steeper than an ASF of 1.22. Also of note is the fact that the ASF peaks before the derivative skewness, meaning slightly closer in the forward direction relative to the nose of the aircraft; while the OASPL peaks when the microphone is at 115° from the nose of the aircraft, the ASF peaks at 122° and the derivative skewness at 130°. The relative angles between the peaks of the statistical metrics agree with previous findings from ground run-up analysis that the ASF peaks more in the forward direction than the derivative skewness, but these angles are roughly 10° more in the forward direction compared to ground run-up data.[8]

This comparison between waveforms from the low and high-power engine conditions reveals a fundamental change in characteristics of the noise as engine power increases. The sharp, compressive shocks present at 150% ETR are noticeably absent at 55%. This analysis, which helps show nonlinear steepening as the source of high-frequency energy at large distance from the source, points to the importance of nonlinear propagation effects in the far field of flyover measurements.

V. DATA ANALYSIS

While the two waveforms examined in detail above provide a basis of discussion for nonlinear characteristics in flyover waveforms, a larger dataset is needed to establish more general trends. The following sections examine the OASPL, derivative skewness, and ASF from the entire course of measurements, featuring five to six flyover events at 40%, 55%, 75%, 100%, and 150% ETR. Statistics are considered from microphones of different sizes, sampling rates, and heights. To present data from all of these conditions, statistics shown are calculated from the 6-dB down region of each waveform.

A. Engine condition

A relatively well-known but important conclusion from the waveform discussion above is that the OASPL increases for higher-power operating conditions. The low-power case had a peak OASPL of 100 dB, and the high-power case peaked at 120 dB. As was also observed, the higher OASPL also results in an increase in nonlinear propagation and the presence of shocks at large distances away from the aircraft. A connection was made between nonlinear propagation and an increase in high-frequency energy in Fig. 3 for two example waveforms. This effect is shown for all spectra from flyover events at engine conditions ranging from 40% ETR to 150% ETR in Fig. 8. Microphone heights ranged from 0 to 91 m and there were five to six flyover events at each engine condition. Individual spectra are shown for each engine condition as thin, lighter lines, while thicker darker lines represent the energetic average from each ETR. Of particular note is the slope of the high-frequency spectrum, in particular

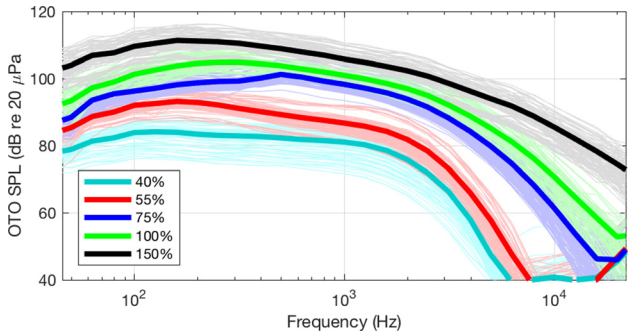

FIG. 8. (Color online) Spectra from the north tower at varying engine condition. Spectra from individual waveforms are shown in lighter lines, while the average at each engine condition is shown in a thicker, darker line.

from 2–6 kHz, which decreases steadily with increasing engine condition, from −70 dB/decade at 40% and 55% ETR to −39 dB/decade at 75%, −31 dB/decade at 100%, and only −21 dB/decade at 150% ETR. This change in high-frequency energy, at distances of over 300 m from the source, shows that with increasing thrust comes an increase in nonlinear effects in the frequency range.

The increase in nonlinear effects with higher engine power is also shown by comparing nonlinearity metrics. The relationship between the increase in OASPL and increases in the nonlinearity metrics can be seen in Fig. 9. The derivative skewness, shown in Fig. 9(a), and the ASF, in Fig. 9(b), are plotted

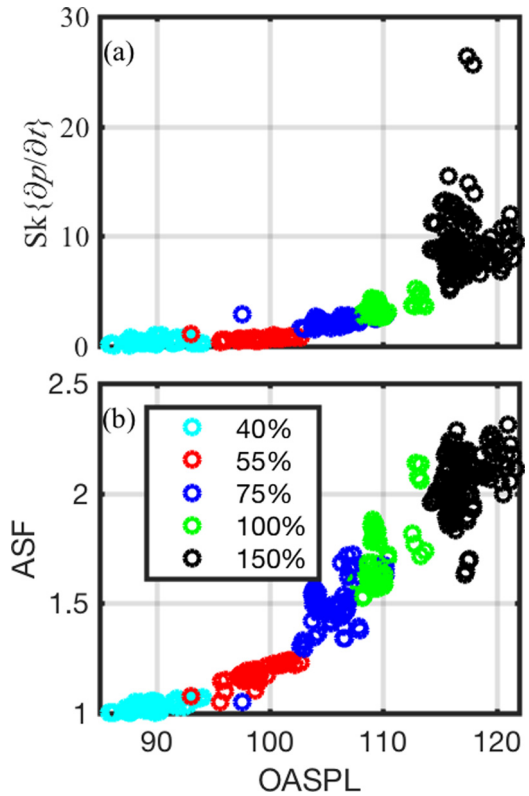

FIG. 9. (Color online) Nonlinearity metrics of waveforms recorded from different flyovers on microphones of different size, specifically the (a) derivative skewness, and (b) ASF. Statistics are calculated from the 6-dB down region of each waveform. The level and derivative skewness values increase with engine condition, and a large spread in derivative skewness values is seen at 150% ETR.

with respect to the OASPL, with statistics calculated from the 6-dB down region of the waveform. A clear trend is seen with increasing OASPL, as both metrics tend to increase. The increase in derivative skewness with OASPL appears almost exponential, with much larger values at 150% ETR than at 100% or below. At 100% and below, derivative skewness values are all below 5. These lower values indicate that significant shocks are not present at this location at 100% ETR and lower.[33] Interestingly, a wide spread of values is observed at 150% ETR, with derivative skewness ranging from 5 to 25. This large range of values could be due to multiple factors, including variations in distance from the aircraft to the microphone, changing weather conditions, a turbulent atmosphere changing shock characteristics,[42,43] natural variation due to the small sample size over which the statistics are calculated, and various measurement considerations. However, in all cases the derivative skewness at 150% exceeds the values seen at lower ETR conditions, suggesting that the most significant shocks are likely to be found when the aircraft is operating at afterburner.

B. Microphone size

The high-frequency energy associated with acoustic shocks may be affected by the frequency response of differently sized microphones.[31,37] For this investigation, waveforms at 150% ETR from two microphones placed 6 in. from each other, one 1/2 in. diameter and the other 1/4 in., allow for an easy comparison between similar waveforms. The similarity between the two microphones is seen in Fig. 10(a), where the waveforms from a 1/4 in. microphone [same as shown in Fig. 5(a)] and its neighboring 1/2 in. microphone are plotted. The waveforms nearly overlay each other, and the PDFs of the pressure waveforms in Fig. 10(b) are nearly identical. This shows that for pressure or level-based measurements, the two microphones are essentially equivalent. However, small differences in the waveforms have a more noticeable impact on a few of the time derivative values in Fig. 10(c), and the PDFs of the waveform derivatives in Fig. 10(d) show differences for the largest derivative values. The waveform from the 1/4 in. microphone exhibits higher derivative values, with some derivative values over 100 $\sigma_{\partial p/\partial t}$, while the highest derivative values from the waveform from the 1/2 in. microphone are at 80 $\sigma_{\partial p/\partial t}$. The presence of larger derivatives in the 1/4 in. microphone show that the largest derivative values associated with acoustic shocks may be underestimated by larger microphones.

Differences in the waveforms due to microphone size also affect nonlinearity indicators. To quantify the effect of microphone size, statistics from 1/4 and 1/2 in. microphones are shown in Fig. 11 as a function of OASPL for multiple flyover tests at engine powers ranging from 15% to 150% ETR, with more than 10 repetitions at each ETR condition. Microphones were included from five heights ranging from 0 to 91.4 m. Although this gives a slight difference in distance between microphones, the largest difference in distance between the microphone at 91.4 m and the microphone at ground level is less than 9 m when the aircraft is flying at 76 m above ground. Statistics are calculated for the 6-dB down region for each microphone and flyover event. Figure 11(b) shows that the derivative skewness measured by the 1/2 in. microphone is

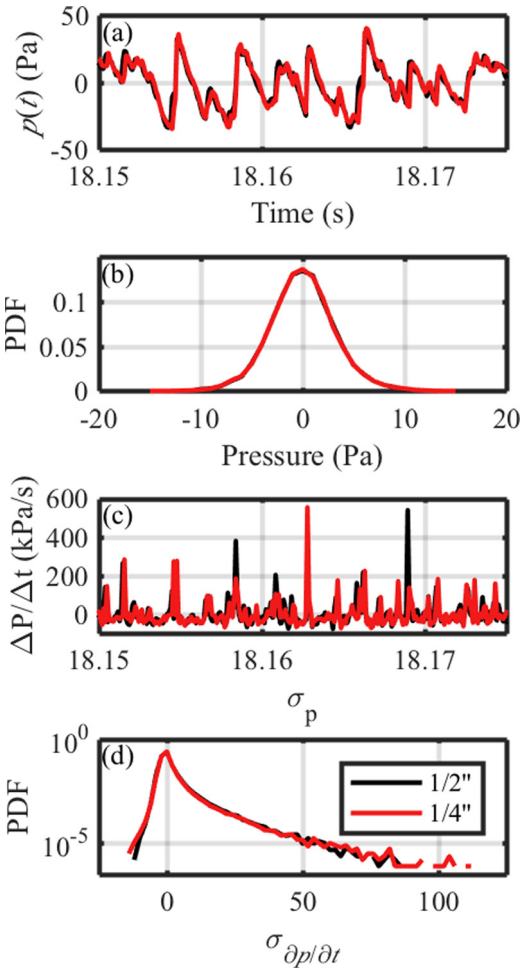

FIG. 10. (Color online) Comparison of (a) a portion of a waveforms, (b) the PDF of the 6-dB down portion of the waveform, (c) the waveform derivatives, and (d) the PDF of the 6-dB down portion of the derivatives from microphones at the same location. The aircraft was operating at 150% ETR.

limited to a value of about 10 while those for the 1/4 in. microphone tend to reach 15 (the small differences seen in the PDF of the derivative in Fig. 10(d) result in higher values for the derivative skewness, which accentuates the presence of outliers). At the highest engine power conditions, near 120 dB OASPL, derivative skewness values peak at 12.5 for the 1/2 in. microphones, while the derivative skewness values from the 1/4 in. microphones reach up to 25. Thus, 1/4 in. microphones (or smaller) should be used to measure high-power jet noise or if the source has a higher peak frequency, as is the case in model-scale jet noise, and in that case rise time is still likely to be limited by transducer size when using 1/4 in. microphones.

It is interesting to note that the difference in microphone size does not appear to affect the ASF, shown in Fig. 11(c). The ASF is a linear average of derivative values, while the derivative skewness is raised to the third power and accentuates the largest derivative values. Therefore, microphone size may be less important if ASF is used to quantify waveform steepness.

The derivative skewness values shown in Fig. 11(a) represent a wide range of values that make a comparison between microphone sizes difficult to quantify. The difference in values

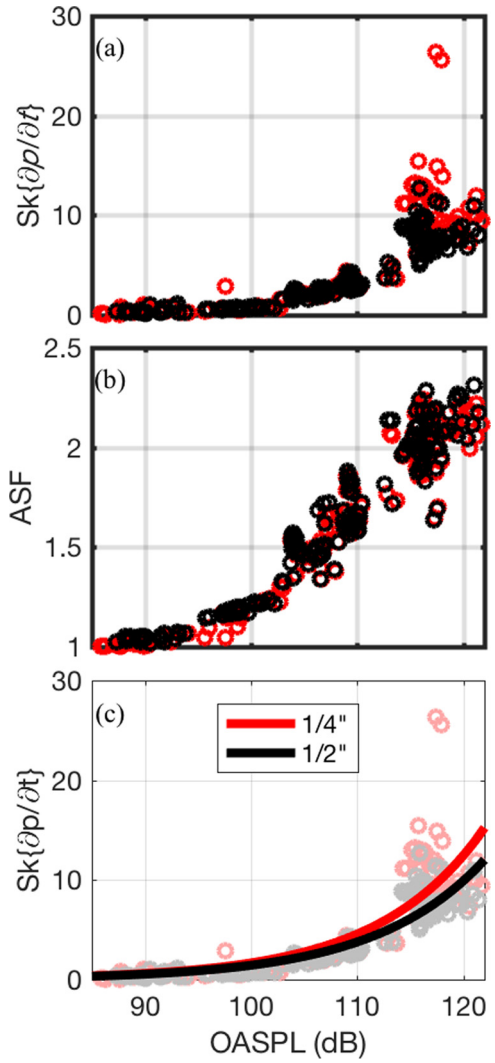

FIG. 11. (Color online) Nonlinearity metrics of waveforms recorded from different flyovers on microphones of different size, specifically the (a) derivative skewness, and (b) ASF. Statistics are calculated from the 6-dB down region of each waveform. (c) The data for each microphone size are fit to curves overlaid on top of the data points.

is much easier to see when the derivative skewness values are fit to a curve. In this case a simple exponential fit is used because it accurately captures the behavior. Two fits were found, one from data recorded using the 1/2 in. microphones, and one from the data recorded using 1/4 in. microphones, and plotted on top of the original data in Fig. 11(c). Though there is a wide spread of values for OASPL > 115, the curve portrays a reasonable average behavior. The two curves are nearly identical below 110 dB, but above this level, which corresponds to the aircraft operating at 150% ETR, they diverge slightly. This difference, while not large, shows that microphone size has a measureable effect on the measurement of high derivative values.

C. Sampling frequency

An important measurement detail that can have a significant impact on the estimation of nonlinearity indicators is sampling frequency. An inadequate sampling frequency not only limits bandwidth, but it also enforces a minimum resolvable rise time that may be insufficient to accurately gauge the nature of some acoustic shocks. To investigate the effects of sampling rate on derivative skewness, the 6-dB down regions of the high and low-power waveforms from Figs. 4(a) and 5(a) have been downsampled to lower sampling rates. The derivative skewness of the resampled waveforms is shown in Fig. 12(a) as a function of the new sampling rate. The 55% ETR case, where the waveform has slightly steepened but contains no significant shocks, was originally sampled at 102.4 kHz while the 150% ETR case was sampled at 204.8 kHz. The low-power measurement, despite the lower sampling rate, accurately captures the steepened nature of the noise, as evident by the fact that resampling yields very little change in derivative skewness until the sampling rate is below 20 kHz. The high-power measurement shows some change even as the sampling rate is lowered from 200 to 100 kHz, as the derivative skewness drops from 8.6 to 8.1. A change this small indicates that a sampling rate of 200 kHz is likely sufficient, but below 100 kHz the derivative skewness drops off more rapidly, with a value of 6.8 at 50 kHz and 4.5 at 20 kHz. Recent work by Reichman *et al.*[33] recommends a sampling rate of roughly 100 times the peak frequency of an initial sinusoid to accurately gauge derivative skewness. However, in this situation, the peak frequency of the noise is 100–200 Hz, and a sampling rate of 100 kHz may still be insufficient to observe the largest shocks. Thus, in the case of high-amplitude broadband noise, the recommendation of sampling at 100 times the peak

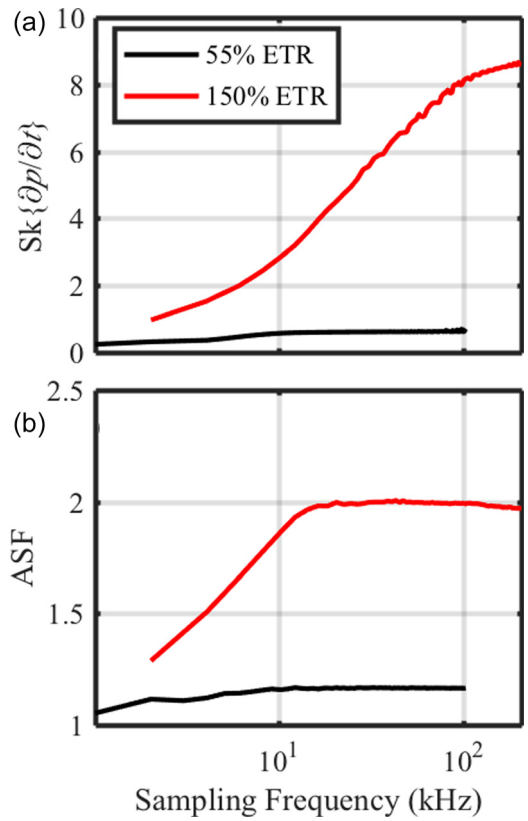

FIG. 12. (Color online) The importance of sampling rate when estimating nonlinear parameters of shock-containing waveforms. The (a) derivative skewness and (b) ASF of the 6-dB down portion of the waveforms from Figs. 4(a) and 5(a) is calculated as the waveforms are resampled to lower sampling rates.

frequency may fall short, and sampling rates of at least 500 times the peak frequency of the noise may be required to accurately calculate the derivative skewness.

While the derivative skewness, with its large emphasis on the steepest shocks, is affected significantly by a reduced sampling rate, the ASF is much more robust. The ASF of the 150% ETR waveform, shown in Fig. 12(b), remains at a nearly constant level as the waveform is downsampled, even to a value of 20 kHz, a tenth of the original sampling rate. This downsampling reduces the derivative skewness by more than a factor of 2, while the ASF is unchanged. Thus the importance of sampling rate depends on the behavior that needs to be identified. While the overall steepness of a waveform can be resolved with lower sampling rate, to accurately capture the largest shocks, sampling rates of 100–200 kHz should be used.

The reduction in derivative skewness due to an inadequate sampling rate can be observed in more than a single waveform. To illustrate this for all data, the data points of derivative skewness as a function of OASPL were fit to an exponential curve, similar to the process used to create Fig. 11(c). All of the represented waveforms were then downsampled, the derivative skewness was calculated from the downsampled waveform, and the data points were again fit to an exponential curve. The curve fits of the downsampled data are shown in Fig. 13(b), for new sampling rates of $f_s = 102.4$, 51.2, 20.5, and 10.2 kHz. Solid lines represent data from 1/4 in. microphones, while dashed lines are from 1/2 in. microphones.

As the sampling rate is reduced from 204.8 to 102.4 kHz for the data from 1/4 in. microphones, only minimal differences are seen at the highest values. Though the individual data points are not plotted here at each sampling rate, it is worth noting that the small changes here occur at only the largest outliers, the points in Fig. 11(c) that have $\mathrm{Sk}\{\partial p/\partial t\} \geq 15$. As the sampling rate is further reduced to 51.2 kHz, a more noticeable decrease at the largest values is observed. Once again, this decrease is due to changes in the larger points in Fig. 13(a), and points that are closer to $\mathrm{Sk}\{\partial p/\partial t\} = 5$ are essentially unaffected by the resampling. For very low sampling rate of 20.5 and 10.2 kHz, drastic reductions in derivative skewness are seen, even for relatively low derivative skewness values. While these low sampling rates are not likely to be seen in practice in full-scale military jet noise, it is worth noting that 10–20 kHz is roughly 100 times the peak frequency of the signal, and thus the earlier recommendation from Reichman *et al.*[33] may fall short for the case of jet noise. The trends observed are similar for 1/2 in. microphones, but with less of a difference between 102.4 and 51.2 kHz. It is important to note that sampling at a sampling rate of 51.2 kHz with a 1/4 in. microphone gives a similar curve to sampling at 204.8 kHz with a 1/2 in. microphone, suggesting that using a large microphone has a similar effect to reducing sampling frequency. In summary, when the amplitude and steepness of the largest shocks must be accurately characterized, such as obtaining an estimate of the derivative skewness, it is important to have a high sampling rate. However, when the ASF or similar metrics are used, sampling rate is less of an issue.

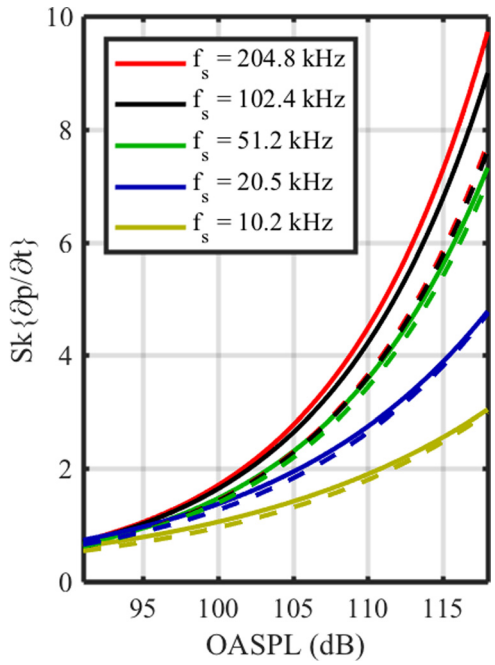

FIG. 13. (Color online) The effects of resampling on trends for derivative skewness with two different microphone sizes. Waveforms were separated according to microphone size and then resampled to various lower sampling rates. Derivative skewness values were fit to a curve and plotted against the OASPL. Solid lines represent data from 1/4 in. microphones, and dashed lines from 1/2 in. microphones. The 204.8 and 102.4 kHz lines for 1/2 in. microphones lie almost directly on top of each other.

D. Height

According to ANSI S12.75-2012, the standard for aircraft flyover measurements, microphones at different heights are used to assess azimuthal directivity.[31] However, because the source and receiver are now both operated above ground there are multi-path interference nulls as well as other possible phenomena that may affect the presence of acoustic shocks. This brings about a need for an analysis of nonlinear indicators as a function of microphone height. The statistics of the 1/4 in. microphones (as shown in Fig. 11) are identified by height in Fig. 14. These statistics appear to be fairly constant for heights between 9.1 and 91 m. The derivative skewness in Fig. 14(a) shows an invariance with height above 9.1 m. At OASPL = 115 dB, the derivative skewness ranges from roughly 5–15, but this variation occurs at all microphone heights. The ASF exhibits a similar behavior as illustrated in Fig. 14(c). The similar values across all heights show that the presence of acoustic shocks is relatively unaffected by measurement height, especially above 9.1 m.

Though the behavior of these statistical metrics appears to be consistent between 9.1 m and 91 m, some slight variations are seen in at the 0 m microphone. One height-dependent trend that is noticeable is the fact that data points measured at 0 m are consistently associated with an OASPL roughly 3 dB higher than other points. The ground microphone measures pressure doubling, as the incident and reflected waves are perfectly coherent across all frequencies, leading to a 6 dB increase compared to a free-field wave. However, the elevated microphone receives both the incident and reflective wave, which are emitted at different times and locations. These

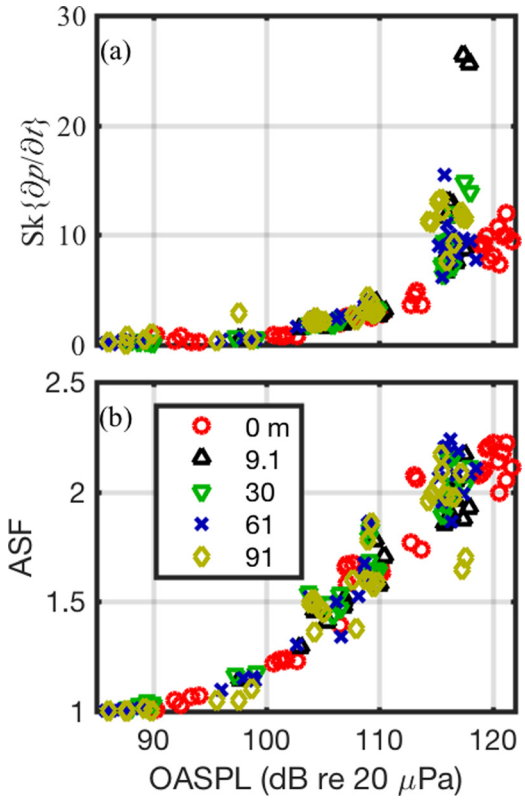

FIG. 14. (Color online) Comparison of the (a) derivative skewness and (b) ASF for varying microphone heights, plotted against OASPL. All data shown are from 1/4 in. microphones, with statistics calculated from the 6-dB down region.

differences result in significantly lower spectral coherence. The resulting spectrum may have interference effects at certain frequencies, but the lower coherence allows their energies to be effectively combined incoherently, which results in an approximate 3 dB increase compared to a free-field wave. Comparing these two different reflection effects provides the observed difference of ~3 dB OASPL between the ground and elevated microphones. For the clusters of points centered at 109 and 117 dB for heights 9.1–91.4 m, the corresponding OASPL of the 0 m microphones is centered at 112 and 120 dB. Though not as noticeable, it appears that some derivative skewness values for the 0 m microphones at 120 dB are slightly lower than corresponding microphones. This behavior has been previously reported by McInerny *et al.*,[30] who showed that some of the largest derivative values were absent at microphones near the ground. This would lead to lower derivative skewness values. However, this behavior affects only the largest shocks, and the ASF is relatively unaffected.

VI. CONCLUSIONS

Acoustic emissions from an F-35 in flight show strong evidence of acoustic shocks due to nonlinear propagation, even at distances of 305 m from the flight path. Statistical measures confirm that slight waveform steepening occurs at low engine power and significant shocks form at high engine power that persist to large distances. The ability to which these acoustic shocks can be accurately characterized depends upon sampling frequency, microphone height, and microphone size. Analysis of these trends leads to three recommendations for future measurements.

First, statistical measures of nonlinearity are relatively constant for heights above 9.1 m. This means that, while directivity concerns may necessitate higher elevated microphone, for the purpose for shock characterizations microphones should be off the ground, but do not need to be higher than 9.1 m. Second, microphone size may limit the minimum resolvable rise time for the largest shocks. In most situations, including spectral content in the audible range, either 1/2 or 1/4 in. microphones may be used. However, if accurate characterization of small rise times is essential, 1/4 in. microphones should be used. Finally, it is recommended that data be sampled at 100–200 kHz. Future work is needed to consider effects of weather-related phenomena, including wind and temperature and their connection to possible turbulence, and to connect nonlinear metrics from ground run-up measurements to metrics from flyover measurements.

ACKNOWLEDGMENTS

The authors would like to acknowledge the helpful comments of an anonymous reviewer, who helped guide additional frequency-domain analysis. The authors would also like to gratefully acknowledge funding for the measurements, provided through the F-35 Program Office and Air Force Research Labs. (Distribution A - Approved for Public Release; Distribution is Unlimited. Cleared 9/26/17; JSF17-943). B.O.R. was funded through an appointment to the Student Research Participation Program at the U.S. Air Force Research Laboratory, 711th Human Performance Wing, Human Effectiveness Directorate, Warfighter Interface Division, Battlespace Acoustics Branch administered by the Oak Ridge Institute for Science and Education through an interagency agreement between the U.S. Department of Energy and USAFRL.

[1]J. E. Ffowcs-Williams, J. Simson, and V. J. Virchis, "'Crackle': An annoying component of jet noise," J. Fluid Mech. **71**, 251–271 (1975).
[2]A. Krothapalli, L. Venkatakrishnan, and L. Lourenco, "Crackle—A dominant component of supersonic jet mixing noise," AIAA Paper 2000-2024 (2000).
[3]D. T. Blackstock, "Nonlinear propagation of jet noise," in *Proceedings of Third Interagency Symposium on University Research in Transportation Noise*, University of Utah, Salt Lake City, Utah (1975), pp. 389–397.
[4]D. F. Pernet and R. C. Payne, "Non-linear propagation of signals in airs," J. Sound Vib. **17**, 383–396 (1971).
[5]C. L. Morfey and G. P. Howell, "Nonlinear propagation of aircraft noise in the atmosphere," AIAA J. **19**, 986–992 (1981).
[6]D. T. Blackstock, "Once nonlinear, always nonlinear," AIP Conf. Proc. **838**, 601–606 (2006).
[7]K. L. Gee, V. W. Sparrow, M. M. James, J. M. Downing, C. M. Hobbs, T. B. Gabrielson, and A. A. Atchley, "Measurement and prediction of noise propagation from a high-power jet aircraft," AIAA J. **45**, 3003–3006 (2007).
[8]K. L. Gee, V. W. Sparrow, M. M. James, J. M. Downing, C. M. Hobbs, T. B. Gabrielson, and A. A. Atchley, "The role of nonlinear effects in the propagation of noise from high-power jet aircraft," J. Acoust. Soc. Am. **123**, 4082–4093 (2008).
[9]B. O. Reichman, K. L. Gee, T. B. Neilsen, S. H. Swift, A. T. Wall, H. L. Gallagher, J. M. Downing, and M. M. James, "Acoustic shock formation in noise propagation during ground run-up operations of military aircraft," AIAA Paper 2017-4043 (2017).
[10]J. N. Punekar, "Numerical simulation of nonlinear random noise," Ph.D. thesis, University of Southampton, Southampton, UK, 1996.

[11]S. Lee, P. J. Morris, and K. S. Brentner, "Nonlinear acoustic propagation predictions with applications to aircraft and helicopter noise," AIAA Paper 2010-1384 (2010).
[12]P. Menounou and D. T. Blackstock, "A new method to predict the evolution of the power spectral density for a finite-amplitude sound wave," J. Acoust. Soc. Am. **115**, 567–580 (2004).
[13]P. Mora, N. Heeb, J. Kastner, E. J. Gutmark, and K. Kailasanath, "Effect of Scale on the far-field pressure skewness and kurtosis of heated supersonic jets," AIAA Paper 2013-0616 (2013).
[14]D. Buchta and J. Freund, "The near-field pressure radiated by planar high-speed free-shear-flow turbulence," J. Fluid Mech. **832**, 383–408 (2017).
[15]S. A. McInerny, "Launch vehicle acoustics. II-Statistics of the time domain data," J. Aircraft **33**, 518–523 (1996).
[16]K. L. Gee, V. W. Sparrow, A. A. Atchley, and T. B. Gabrielson, "On the perception of crackle in high-amplitude jet noise," AIAA J. **45**, 593–598 (2007).
[17]B. Greska and A. Krothapalli, "On the far-field propagation of high-speed jet noise," in *Proceedings of ASME 2008 Noise Control and Acoustics Division Conference* (2008), pp. 129–133.
[18]W. J. Baars and C. E. Tinney, "Shock-structures in the acoustic field of a Mach 3 jet with crackle," J. Sound Vib. **333**, 2539–2553 (2014).
[19]M. B. Muhlestein, K. L. Gee, T. B. Neilsen, and D. C. Thomas, "Evolution of the average steepening factor for nonlinearly propagating waves," J. Acoust. Soc. Am. **137**, 640–650 (2015).
[20]M. Muhlestein and K. Gee, "Experimental investigation of a characteristic shock formation distance in finite-amplitude noise propagation," Proc. Mtgs. Acoust. **12**, 045002 (2011).
[21]M. M. James, A. R. Salton, J. M. Downing, K. L. Gee, T. B. Neilsen, B. O. Reichman, R. L. McKinley, A. T. Wall, and H. L. Gallagher, "Acoustic emissions from F-35 aircraft during ground run-up," AIAA Paper 2015-2375 (2015).
[22]R. H. Schlinker, S. A. Liljenberg, D. R. Polak, K. A. Post, C. T. Chipman, and A. M. Stern, "Supersonic jet noise source characteristics and propagation: Engine and model scale," AIAA Paper 2007-3623 (2007).
[23]E. Zwieback, "Flyover noise testing of commercial jet airplanes," J. Aircraft **10**, 538–545 (1973).
[24]U. Michel and A. Michalke, "Prediction of flyover jet noise spectra from static tests," J. Acoust. Soc. Am. **68**, S105 (1980).
[25]A. Krothapalli, P. Soderman, C. Allen, J. Hayes, and S. Jaeger, "Flight effects on the far-field noise of a heated supersonic jet," AIAA J. **35**, 952–957 (1997).
[26]R. Schlinker, J. Simonich, and R. Reba, "Flight effects on supersonic jet noise from chevron nozzles," AIAA Paper 2011-2703 (2011).
[27]J. Seiner, B. Jansen, and L. Ukeiley, "Acoustic fly-over studies of F/AE/F aircraft during FCLP mission," AIAA Paper 2003-3330 (2003).
[28]U. Michel, "Prediction of jet mixing noise in flight from static tests," in *Proceedings of 22nd AIAA/CEAS Aeroacoustics Conference* (2016), p. 2807.
[29]K. L. Gee, T. B. Neilsen, M. Downing, M. M. James, and S. A. McInerny, "Characterizing nonlinearity in jet aircraft flyover data," Proc. Mtgs. Acoust. **12**, 040008 (2013).
[30]S. McInerny, K. L. Gee, M. Dowing, and M. James, "Acoustical nonlinearities in aircraft flyover data," AIAA Paper 2007-3654 (2007).
[31]ANSI S12.75-2012, "Methods for the measurement of noise emissions from high performance military jet aircraft," AIAA J. **47**, 186–194 (2009).
[32]S. A. McInerny, M. Downing, C. Hobbs, M. James, and M. Hannon, "Metrics that characterize nonlinearity in jet noise," AIP Conf. Proc. **838**, 560–563 (2006).
[33]B. O. Reichman, M. B. Muhlestein, K. L. Gee, T. B. Neilsen, and D. C. Thomas, "Evolution of the derivative skewness for nonlinearly propagating waves," J. Acoust. Soc. Am. **139**, 1390–1403 (2016).
[34]J. Gallagher, "The effect of non-linear propagation in jet noise," in *AIAA 20th Aerospace Sciences Meeting* (1982).
[35]K. L. Gee, T. B. Neilsen, J. M. Downing, M. M. James, R. L. McKinley, R. C. McKinley, and A. T. Wall, "Near-field shock formation in noise propagation from a high-power jet aircraft," J. Acoust. Soc. Am. **133**, EL88–EL93 (2013).
[36]B. O. Reichman, A. T. Wall, K. L. Gee, T. B. Neilsen, J. M. Downing, M. M. James, and R. L. McKinley, "Modeling far-field acoustical nonlinearity from F-35 aircraft during ground run-up," AIAA Paper 2016-1888 (2016).
[37]T. B. Gabrielson, T. M. Marston, and A. A. Atchley, "Nonlinear propagation modeling: Guidelines for supporting measurements," J. Acoust. Soc. Am. **118**, 1873–1874 (2005).
[38]http://www.gras.dk/products/measurement-microphone-cartridge/prepolarized-cartridges-0-volt/product/159-40bd (Last viewed 1/26/2018).
[39]http://www.gras.dk/products/measurement-microphone-sets/constant-current-power-ccp/product/141-46ao (Last viewed 1/26/2018).
[40]J. S. Bendat and A. G. Piersol, "Probability fundamentals," in *Random Data: Analysis and Measurement Procedures* (Wiley, Hoboken, NJ, 1986).
[41]K. L. Gee and V. W. Sparrow, "Quantifying nonlinearity in the propagation of noise from military jet aircraft," Noise-Con Proc. **114**, 397–404 (2005).
[42]A. D. Pierce, "Statistical theory of atmospheric turbulence on sonic boom rise times," J. Acoust. Soc. Am. **49**, 906–924 (1971).
[43]B. Lipkens and D. Blackstock, "Model experiment to study sonic boom propagation through turbulence. Part I: General results," J. Acoust. Soc. Am. **103**, 148–158 (1998).